Available online at www.sciencedirect.com
SCIENCE DIRECT®
Journal of Magnetic Resonance 164 (2003) 351–357
JMR Journal of Magnetic Resonance
www.elsevier.com/locate/jmr

Ghost-peak suppression in ultrafast two-dimensional NMR spectroscopy

Yoav Shrot and Lucio Frydman*

Department of Chemical Physics, Weizmann Institute of Science, 76100 Rehovot, Israel

Received 14 April 2003

Abstract

Two-dimensional (2D) spectroscopy is central to many contemporary applications of NMR. Recently, we have introduced a new approach whereby 2D NMR spectra can be collected within a single scan. This methodology employs a magnetic field gradient in order to spatially encode the time evolution occurring along the indirect dimension. The discrete nature of the t_1 incrementation and its one-to-one correspondence with the spatial encoding, may lead to a number of artifacts. Most notable among these is a periodicity of the spectral peaks that are observed along the indirect axes. The appearance of such 'ghost-peaks', which may sometime coincide with genuine cross-peaks, could hamper a proper interpretation of the spectra. This contribution reviews the origin of such multiple resonances, and proposes a procedure for their elimination based on the acquisition of a small number of complementary scans. Such complementary scans can be simultaneously employed for the sake of phase-cycling out other unwanted signals, and improve the overall indirect-domain spectral resolution. Brief mathematical descriptions of the ghost-peak generation and ghost-peak suppression mechanisms are described, followed by experimental tests on a number of samples using various pulse sequences.

Keywords: Two-dimensional spectroscopy; Ultrafast acquisitions; Ghost-peaks; Artifact suppression; Resolution enhancement

1. Introduction

Multidimensional spectroscopy constitutes one of the cornerstones supporting the chemical, biological, and clinical applications of NMR [1]. Two-dimensional (2D) NMR spectra in particular, provide a routine approach to the assignment of peaks and to the establishment of connectivities between neighboring chemical sites [1–4]. The main complication in extending the dimensionality of a given NMR experiment lies in the relatively longer times that will then be needed for the acquisition of the data. This demand originates from the manner in which multidimensional NMR experiments are implemented [5–7]: the signal arising along one of the spectral dimensions is directly monitored over a few hundred of milliseconds in the usual pulsed NMR fashion [8], whereas the spins' evolution along the remaining time axes is indirectly monitored via a discrete incrementation of their associated time-domain variables. Collecting an N-dimensional NMR spectrum will therefore require monitoring a large array of independent signals—one for each of the points making up the $(N-1)$ indirect dimensions—resulting in an exponential increase of the experimental acquisition time with N.

Very recently we proposed and demonstrated an alternative method for carrying out multidimensional NMR experiments, that is capable of gathering the complete set of spectral information within a single scan [9–11]. This new methodology is based on replacing the serial acquisitions usually carried out to monitor signals along various indirect time-dimensions, by a parallelized encoding of the spin evolution. The essence of this method as it applies to the ultrafast acquisition of 2D NMR spectra, is conveyed in Fig. 1. At the core of this methodology lies the application of a magnetic field gradient which, together with a train of spatially selective excitation pulses, endows spins at different positions within the sample with incremented values of their indirect t_1 evolution times. As this excitation gradient is

* Corresponding author. Fax: +972-8-9344123.
E-mail address: lucio.frydman@weizmann.ac.il (L. Frydman).

1090-7807/$ - see front matter © 2003 Elsevier Inc. All rights reserved.
doi:10.1016/S1090-7807(03)00177-0

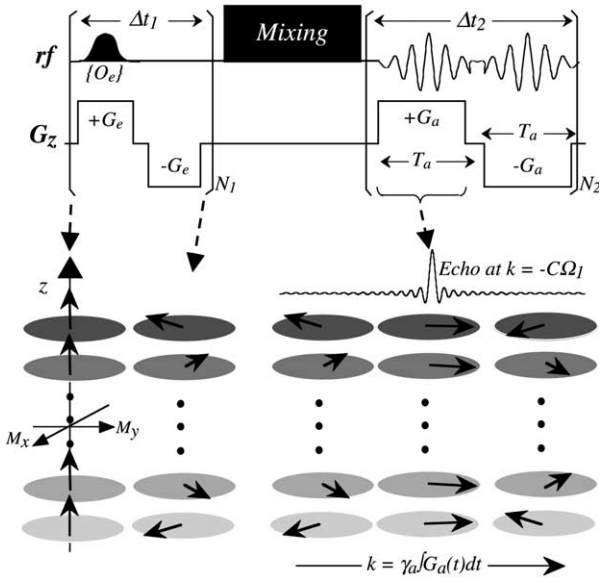

Fig. 1. General pulse scheme and physical principles involved in the collection of 2D NMR spectra within a single-scan. A train of N_1 frequency-shifted pulses is applied in the presence of a field gradient G_e to achieve a sequential excitation of spins throughout different positions in the sample (left). Following a mixing sequence data are collected while in the presence of an oscillating acquisition gradient $\pm G_a$, capable of repetitively unwinding and winding the shift-induced spiral of spin-packets encoded during the excitation. The sharp echoes that are then generated unveil an array of spectra along the indirect dimension, modulated along t_2 according to their evolution frequencies.

applied in a time-reversed echoing fashion, no phase related to the spatial position of the spins is explicitly imprinted onto the spins. Only an internal $\Omega_1 t_1$ phase factor is thus accrued at the conclusion of the evolution, leading to a shift-induced winding of the spin coherences along a spatial coordinate. This indirect-domain information is preserved throughout the mixing process, and subsequently decoded by means of an acquisition gradient applied while the signal from the spins is being recorded. Such gradient can unwind the helix of spin-packets that was created during the course of the initial t_1 evolution time, and lead to an observable echo signal. The timing of this echo will depend on the strength of the Ω_1 internal interaction that wound the spin-packets prior to the mixing, hence allowing one to map the spectrum along the indirect domain. Furthermore, this unwinding process can be immediately reversed and then repeated multiple (N_2) times by alternating the sign of the acquisition gradient, thereby allowing one to monitor the Ω_2 frequencies of the spins active during the second, directly-detected t_2 period. Signals obtained during such cyclic rephasing/dephasing train can be arranged into a bidimensional data set, which by Fourier analysis along t_2 will lead to the desired 2D NMR spectrum correlating Ω_1 and Ω_2 frequencies. The incorporation of multiple linearly independent gradient geometries also enables an extension of this protocol to arbitrary N-dimensional experiments, where frequencies along $N-1$ indirect domains are spatially encoded and the final time-domain is monitored in the usual direct fashion [11].

A curious aspect of the ultrafast acquisition modality summarized in the paragraph above, is its apparent forfeiting of the Fourier transformation (FT) along the indirect domain. Indeed frequencies Ω_1 do not end up revealed after the analysis of a time-modulated signal, but through changes in the timing of a constructive echo built up by spin-packets associated to different spatial positions. In fact, however, it is possible to trace this absence of an explicit FT to the presence of two conjugate Fourier processes that take place one after the other: one is the initial spatial encoding of the spin-packets driven by the frequency-selective RF pulses, the second is the final decoding of the internal Ω_1 evolution by means of the acquisition gradient. Furthermore, as in many other instances involving Fourier processes [12,13], also in the case of ultrafast NMR will such procedures become associated with a number of artifacts. Most noticeable among these are the presence of minor peaks flanking the main echoes along the indirect-domain axis, and which may complicate the interpretation of the spectra. We refer to such additional coherence echoes as "ghost-peaks"; to review their origin and to propose and exemplify methods for their suppression, are the main purposes of the present manuscript.

2. Peaks and ghosts: origin and suppression

Fig. 2a rationalizes the origin of the ghost-peaks appearing along the indirect dimension of ultrafast experiments, using the signal acquisition stage of a simplified "5-sliced" spin-packet profile as an example. As spin-packets are assumed here excited by a progression of RF pulses spaced at constant frequency increments ΔO_e, they will find themselves within slices positioned at equal distances Δz from one another. Hence upon being acted during the course of the acquisition by a gradient G_a, their precession offsets will once again be spaced by a constant difference ΔO_a. Because of this equi-distance in the spin-packets' precession frequencies their coherent echoing will occur not once but multiple times, at timings dictated by the precession frequency Ω_1 as well as by the $1/(\Delta O_a)$ interval. All such echo peaks should in principle have the same intensity; however, this is rarely the case, due to the dephasing that spins within each of the discrete spin-packets experience upon being acted by a gradient. A realistic ghosting situation in ultrafast ^{1}H NMR experiments is thus more as reflected by the cartoon on Fig. 2b, which shows one main (or ghost) peak flanked by one or two minor resonances.

Under optimal conditions involving sufficiently intense magnetic field gradients, short Δt_1 dwell times, etc.,

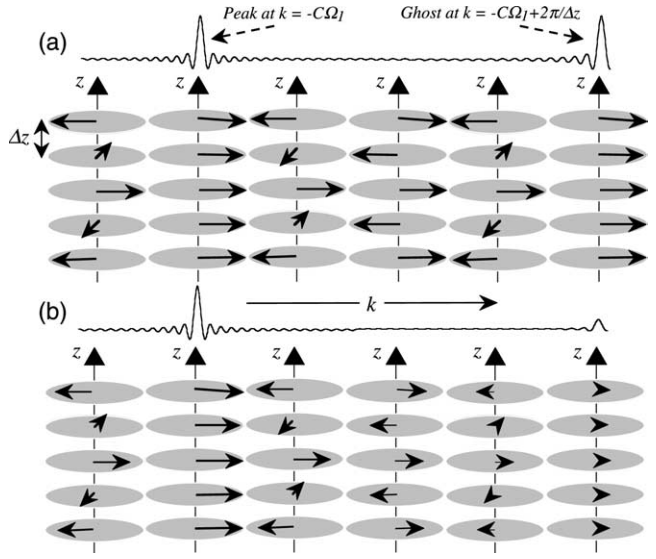

Fig. 2. (a) Idealized origin of the ghost-peaks arising along the indirect dimension of 2D ultrafast NMR experiments. The fact that all spin-packets are equally spaced implies that their relative resonance offsets are multiples of some basic difference ΔO_a, and consequently will come into constructive interference repetitive times at time intervals given by $1/(\Delta O_a)$ (or speaking in k-axis units, in multiples of $2\pi/\Delta z$). (b) Actual intensity pattern expected from main- vs. ghost-peaks in ultrafast NMR experiments. The differences in relative intensities vis-á-vis (a) result from intra-slice rephasing/dephasing processes imparted by G_e and G_a, illustrated by a variation in the spin-packet intensities with time. The actual ratio between the peak and ghost intensities depends on details of the sample's excitation [10].

ghost-peaks flanking the main resonances can always be placed outside the spectral region of interest. In such cases, they will not be a complication. In other instances, particularly when dealing with weak gradients, lower-γ nuclides or large chemical shift ranges, the full indirect-domain region of interest may be hard to cover and ghost-peaks can become useful aids for including within a given spectral region all the potential resonances. One might then wish to preserve them. Still, other situations might arise where ghost-peaks appear as minor artifacts within a spectral region containing main peaks of interest from other chemically inequivalent sites. In such scenario ghost-peaks constitute a nuisance worth getting rid of; their suppression is the focus of the remainder of this work.

As follows from the analysis in Fig. 2, the origin of ghost-peaks can be traced to the uniform frequency spacing imparted by the excitation pulse train upon partitioning the sample into discrete spin-packets. This uniform spacing is in turn a consequence of relying on a constant Δt_1 separation for the interval elapsed between the excitation of contiguous slices, a demand that can itself be traced to the constraints placed by the fast FT algorithm that is involved in the canonical scheme of 2D NMR spectroscopy. On the other hand, the fact that our ultrafast schemes do not rely on this numerical transformation altogether, lifts the demand for a constant Δt_1 incrementation. Then, provided that spins are still excited at positions corresponding the desired winding of spin-packets (i.e., that a linearity in the position vs. t_1 dependence is maintained), any sampling of the $\Omega_1 t_1$ evolution phases will still provide a main echo peak at the expected position. By contrast ghost-peaks flanking this main echo should disappear whenever the Δt_1 periodicity is broken, as the ΔO_a frequency separation that brought about their generation is no longer there. The numerical calculations in Fig. 3, which illustrate the indirect-domain line shapes arising upon departing from the usual linear sampling of the t_1 evolution, validate these expectations. Yet at the same time, they point out a number of pitfalls which may make a non-uniform sampling approach impractical in a majority of single-scan applications. Foremost among these is the increased noise that will characterize such spectra, a consequence of the numerous partially constructive interference conditions which are met when relying on a non-uniform excitation of the spin-packets. Compounding this problem are the large segments of sample remaining outside the regions of excitation (and

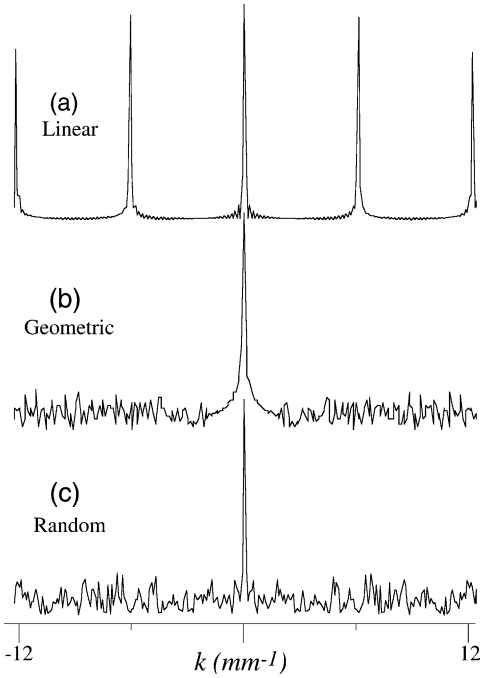

Fig. 3. Line shapes describing the echoes expected along the indirect dimensions of single-scan 2D NMR experiments when executing (a) a linear incrementation in the t_1 experienced by spins in the various slices; (b) a geometric t_1 incrementation of the slices; (c) random Δt_1 changes. In all cases the excitation offsets were varied according to the t_1 demands by keeping the $\Delta t_1/\Delta O_e$ ratio constant, implying that the pitch imparted by Ω_1 on the spin-packet's winding throughout the sample was the same for all cases. All plots are given in magnitude representation and were numerically calculated assuming 95 N_1 initial excitation slices, a 1.5 cm sample length, $\Omega_1 = 0$, and no intra-slice dephasing.

henceforth lost to the experiment), as well as the serious demands that such a procedure would made on the hardware upon exciting the spin-packets in the regions of closest spacing.

In view of these practical limitations we decided to explore an alternative that is also capable of eliminating ghost-peaks in ultrafast acquisitions, while relying on the original (and easier to implement) equi-spaced excitation scheme. This alternative is based on the realization that a decrease in the effective ΔO_a separation between the spin-packet's offsets, will assist in furthering away the artifact's position. Although the minimum offset separation that can be achieved in a given experiment is limited by the actual characteristics of the hardware, it is always possible to artificially half the effective separation between slices by combining two complementary sets of experiments where their respective excitation offsets have been shifted by $\Delta O_e/2$. Leaving all remaining parameters in the sequence unchanged will not suffice to give a spectrum that is free from every other ghost unless a correction is also made for the $\Omega_1 \Delta t_1/2$ difference in phase that should also characterize both experiments. Fig. 4 summarizes the resulting change that should then be used in the excitation offset and in the t_1 timing of both experiments, for achieving a proper elimination of every other ghost-peak. Evidently, if a need were to arise, an arbitrary number M of independent experiments could be combined along these guidelines in order to eliminate $(M-1)$ adjacent ghost-peaks.

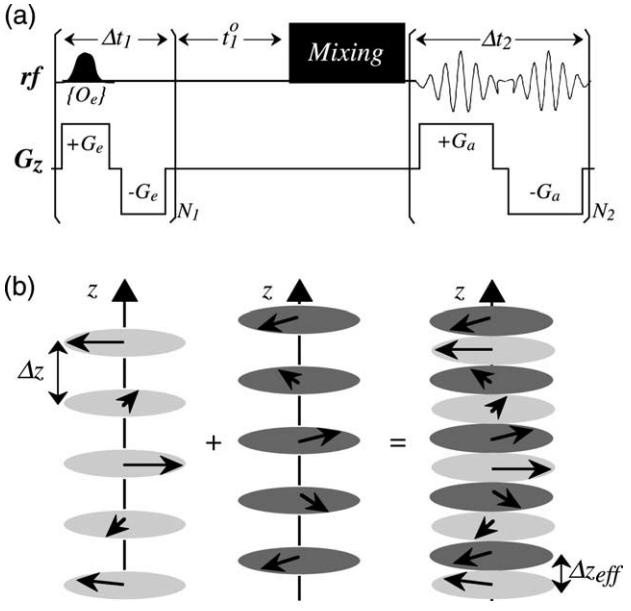

Fig. 4. Pulse sequence proposed for the elimination of ghost-peaks in ultrafast 2D NMR (a), and pictorial description of how the pulse sequence reduces the effective separation between the excited slices (b) assuming a two-scan cycling with $\Omega_1 \neq 0$. The controlled incrementation in the position and the timing used in the excitation, defined in turn by the t_1^0 delay and the $\{O_e\}$ offset series used in the excitation of each experiment, effectively allows one to double the number of slices used to encode the indirect-dimension evolution.

Having given an overview on the origin of ghost-peaks in ultrafast NMR and a physical description of procedures that could suppress them, we turn now to a brief mathematical justification of these matters. We base such analysis on the scenario depicted in Fig. 1a, where the t_1 evolution is triggered by a train of N_1 frequency-shifted RF pulses, applied in conjunction with a gradient that for simplicity we shall assume longitudinal along the z-axis. As a result of these choices spin-packets within each of the excited slices will end up having identical magnitudes, but will be affected by different t_1 evolution times. Neglecting for simplicity relaxation as well as the intra-slice dephasing brought about by the action of the gradients (responsible in turn for the enveloping of the peaks depicted in Fig. 2b), we can write the overall magnetization arising at the conclusion of the evolution period as the discrete sum over slices

$$M = \frac{A}{N_1} \sum_{j=0}^{N_1-1} e^{i\Omega_1 t_1(j)}, \tag{1}$$

where A is the overall magnetization from a particular chemical site over the whole sample, and t_1's slice-dependence can be summarized as $t_1(j) = j \cdot \Delta t_1 + t_1^0$ (the purpose of keeping t_1^0 as an explicit parameter is to implement later the scheme in Fig. 4). Following the mixing period and during the course of the acquisition a gradient G_a is applied, which will affect spins differently depending on their actual z positions. Each of the spin-packets will then accumulate a phase factor which can be described as $k \cdot z$, k being the $\gamma_a \int_0^t G_a(t')\,dt'$ wavenumber that will eventually become the frequency axis of the indirect domain. The signal collected for each particular $\pm G_a$ cycle (corresponding to the signal for a particular t_2 value, cf. Fig. 1) can then also be written as the sum over discrete slices

$$S(k) = \frac{A}{N_1} \sum_{j=0}^{N_1-1} e^{i\Omega_1 t_1(j)} e^{ik \cdot z(j)}. \tag{2}$$

Once again the slice-dependence of the z positions can be summarized as $z(j) = j \cdot \Delta z + z^0$. Replacing both the temporal and spatial j-dependencies into Eq. (2) leads to

$$S(k) = \frac{A}{N_1} e^{i\left(\Omega_1 t_1^0 + kz^0\right)} \sum_{j=0}^{N_1-1} e^{i(\Omega_1 \Delta t_1 + k\Delta z)j}. \tag{3}$$

It is clear from this equation that if a sufficiently large number N_1 of slices is chosen, no $S(k)$ signal will be observable unless the $\Omega_1 \Delta t_1 + k\Delta z$ argument inside the sum is made an integer multiple of 2π. Since both Δt_1 and Δz are fixed parameters of the experiment, this requirement implies that echoes generated by the constructive interference among all the slices will only arise when

$$k = -\Omega_1 \cdot \frac{\Delta t_1}{\Delta z} + n \cdot \frac{2\pi}{\Delta z}; \quad n = 0, \pm 1, \pm 2, \ldots \tag{4}$$

This in turn is a central relation in ultrafast NMR, as it shows that the k variable activated during the acquisition is capable of mapping through a constructive interference phenomenon the internal evolution frequencies that were active prior to the mixing period. In this sense we often refer to the k-axis as to the v_1 dimension of the 2D NMR spectrum, the spatio-temporal ratio $C = \Delta t_1/\Delta z$ relating the actual scales of the two.

Eq. (4) indicates that in addition to the main constructive interference occurring at $k = -C\Omega_1$ other echoes will also form along the k-axis, centered at this chemical shift position and spaced at constant intervals of $2\pi/\Delta z$. These multiple echoes are naturally the ghost-peaks referred to in the preceding paragraphs. In order to demonstrate that the addition of suitably timed, complementary acquisitions can eliminate any one of these ghost-peaks, it is convenient to derive next the actual complex amplitude defining ghost-peaks. This can be done by replacing the nth echo condition defined by Eq. (4) into the signal expression given in Eq. (3), to obtain:

$$S(k_n) = A e^{i\Omega_1\left(-\frac{\Delta t_1}{\Delta z}z^0 + t_1^0\right)} e^{i2\pi n \frac{z^0}{\Delta z}}. \tag{5}$$

If now P-independent experiments are carried out where the Ω_1-independent arguments in the phase expression of Eq. (5), z^0 and t_1^0, are altered by increments of $[(\Delta z)/P]$ and $[(\Delta t_1)/P]$, respectively, then the sum of all the resulting P signals will yield:

$$S(k_n) = A e^{i\Omega_1\left(-\frac{\Delta t_1}{\Delta z}z^0 + t_1^0\right)} e^{i2\pi n \frac{z^0}{\Delta z}} \sum_{l=1}^{P} e^{i2\pi n \frac{l}{P}}. \tag{6}$$

It then follows that repeating the experiment P times with the proper incrementation of the spatial and temporal phases, will zero the nth ghost-peak's amplitude unless n equals an integer multiple of P. In other words the combination of two complementary scans will succeed in eliminating every other echo-peak, three complementary acquisitions can eliminate two consecutive ghost-peaks, etc. Eq. (6) thus provides the mathematical basis for the arguments exemplified in Fig. 4. Such arguments also indicate that the effective spectral width along the indirect domain remains unaffected by the ghost suppression, given the constant $\Delta t_1/\Delta z$ ratio characterizing the single- and multiple-scan acquisitions.

3. Results and discussion

In order to verify the performance of the concepts introduced in the preceding section, a series of experiments designed to suppress odd ghost-peaks by combination of two suitably cycled 2D NMR scans were carried out. Towards this end conditions conducive to the formation of ghost-peaks were set on a Bruker Avance 500 MHz NMR spectrometer, equipped with a Nalorac TXI single-axis gradient probehead. Following the calibration of the gradient's maximum strength ($G \approx 69$ G/cm), typical switching times ($\sim$10 μs) and the sample's dimension ($\approx$1.5 cm), the pulse sequence in Fig. 4 was programmed to obtain both ghost-affected as well as ghost-free 2D NMR spectra. Fig. 5a presents a mixing-less single-scan 2D NMR spectrum thus collected on an n-butylchloride/$CDCl_3$ sample, clearly showing the appearance of first-order ghost-peaks along the indirect domain which flank the four resonances expected along the main diagonal. Implementation and co-addition of a second scan where the initial delay period is shifted by $[-(\Delta t_1)/2]$ whereas the spatial position of the various spin-packets is displaced by shifting the offset frequencies employed in the excitation by

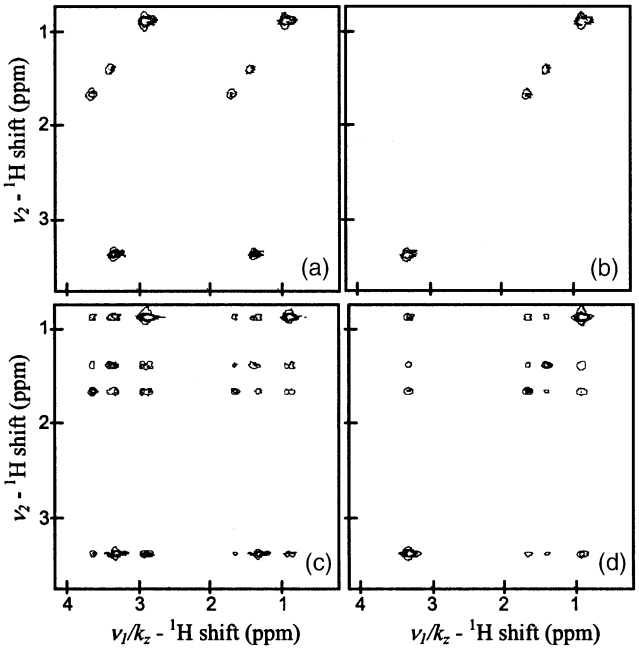

Fig. 5. Exemplification of the odd-suppression procedure based on 2D NMR spectra acquired on an n-butylchloride/$CDCl_3$ sample. (a) Single-scan spectrum acquired in the absence of a mixing process. (b) Two-scan counterpart illustrating the suppression of ghost-peaks and the appearance of peaks only along the main diagonal. (c, d) Idem as (a, b), but incorporating a 70 ms long WALTZ-based mixing sequence [14,16] between the t_1 and t_2 periods. Excitation parameters in all these experiments included forty 400 μs long rectangular $\pi/2$ pulses, applied at $\Delta O_e = 8$ kHz offset increments while in the presence of a 175 kHz/cm z gradient. The acquisition involved 128 N_2 gradient echoes with $G_a = 145$ kHz/cm, scanned with $T_a = 310$ μs (plus 10 μs gradient switching times) and a 5 μs physical dwell time. These conditions yielded 16k points in the $(\nu_1/k, t_2)$-domain. For their spectral presentation these data were sorted out as described in [9,10], linear predicted in the time domain to 128×256 points, FT back into the 2D frequency domain, and presented in magnitude mode. For the ghost-suppression experiments in (b) and (d), all the selective pulses' frequencies were displaced by 4 kHz and the t_1^0 delay following the excitation was decreased by 470 μs.

$[-(\Delta O_e)/2]$, leads to the ghost-free results presented in Fig. 5b. As a further test on the usefulness of this approach the same test was repeated on a TOCSY experiment incorporating an isotropic mixing period between t_1 and t_2 [14]. As can be appreciated by comparing the single- and two-scan results presented in Figs. 5c and d, the suppression that can be achieved of the ghost-peaks is nearly complete.

As an additional example of the ghost-suppression method, Fig. 6 presents a series of parallel tests carried out on a DL-phenylalanine/D_2O solution. Once again, the results of the mixing-less as well as of the TOCSY-based experiments demonstrate the effectiveness of the ghost elimination technique. An interesting feature to note on the TOCSY spectrum of this solution is the small group of echoes appearing in the single-scan experiment next to the phenyl group peaks, and marked by an asterisk in Fig. 6c. At first glance the positions of these echoes do not match the positions expected from either the ghosts of the aliphatic peaks or from TOCSY cross-peaks. The suppression procedure, however, reveals that these are indeed ghost-peaks. The reason for their unusual spectral location lies in the fact that they actually arise from the coherence transfer pathway that is opposite to the one giving origin to the main peaks in the spectrum. Indeed like most mixing sequences, the TOCSY mixing converts the phase encoding generated during the initial t_1 evolution into an amplitude-modulated signal [3,7,15]. Only one of the two ensuing coherence pathways, however, is chosen by the acquisition gradient to yield the refocusing echoes denoted by the condition in Eq. (4). The constructive peaks arising from the remaining coherence transfer pathway will usually be invisible under normal conditions, their signals being dephased away by the gradients. On the other hand, their associated ghost-peaks might still be observable. In fact the minor peaks appearing adjacent to the phenyl resonance in the TOCSY spectrum of Fig. 6c can be traced to first-order ghosts arising from the phenyl peak's mirror-imaged spectrum; being odd-numbered artifacts, these minor peaks are also efficiently eliminated by the ghost-suppression procedure.

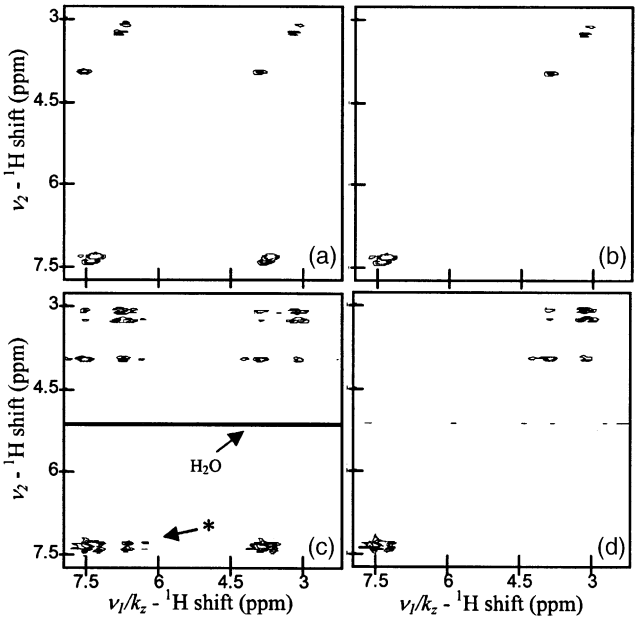

Fig. 6. Exemplification of the odd ghost-suppression procedure on a DL-phenylalanine/D_2O solution. (a) Single-scan 2D ^{1}H NMR spectrum; no mixing. (b) Two-scan spectrum with ghost suppression. (c) Idem as (a) but based on a TOCSY experiment incorporating a 65 ms long WALTZ sequence. (d) Two-scan ghost-suppressed TOCSY experiment. In all cases water presaturation was implemented prior to the actual pulse sequence by an on-resonance low-level 1.2 s irradiation pulse (still, the horizontal line in certain panels is due to imperfections in the water suppression). Excitation and acquisition parameters were as in Fig. 5 except for the use of 250 μs long selective pulses and of $T_a = 190$ μs. These conditions yielded 10k points in the $(\nu_1/k, t_2)$-domain, which were processed as in Fig. 5. The ghost cycling involved an offset shift in all excitation pulses of 4 kHz, along with a t_1^0 delay change of −280 μs. The asterisk marks spectral ghosts arising from ν_1 reflections of the phenyl peaks (see text).

4. Conclusions

The main aim of the present paper was to give a description about the origin of ghost-peaks in ultrafast multidimensional NMR, and to introduce a method for suppressing these peaks. The principles underlying the suppression are relatively simple, and the method's implementation straightforward. This does not necessarily mean that the suppression of ghost-peaks is "a must" in ultrafast NMR experiments, or that it is even an aim which will invariably be desired. In fact if moderately strong gradients are available, their appearance in most homonuclear ^{1}H NMR spectroscopy settings can be managed to relatively small and tolerable intensity levels. Although we have not found this to be the case in a majority of heteronuclear experiments, the presence of ghost-peaks might be desirable even in these cases as a mean for "folding-in" resonances which would otherwise lie outside the spectral range that can be explored. On the other hand one could envision several scenarios (including spectroscopic imaging) where the absence of intense enough gradients makes ghost-peaks a complication worth suppressing. Two different routes were thus discussed in this paper for the suppression of these ultrafast NMR artifacts: one which preserves the single-scan nature of the experiment but sacrifices even further its signal-to-noise ratio, another which does not compromise in sensitivity but relinquishes its single-scan nature. None of these seem ideal solutions, and hence the search for other ghost-suppression mechanisms is likely to continue. On the other hand it is worth pointing out that several instances arise where the acquisition of a 2D NMR experiments in two scans is desirable for the sake of suppressing other, non-ghost kind of artifacts.

This is particularly common if the spectra being sought are to be recorded in the presence of an intense background signal (e.g., H_2O), susceptible to elimination by a 180° phase-cycling of the initial train of excitation pulses. Such phase-cycling away of unwanted background signals can be implemented concurrently with the ghost-peak suppression protocol put forward in Fig. 4, to achieve elimination of both kind of artifacts within a single pair of scans. No increase in the overall acquisition time of the experiment will then result.

Acknowledgments

We thank Dr. Adonis Lupulescu for insightful discussions. This work was supported by the Philip M. Klutznick Fund for Research, the Minerva Foundation (Munich, FRG), as well as by a grant from the Henry Gutwirth Fund for the Promotion of Research.

References

[1] D.M. Grant, R.K. Harris (Eds.), Encyclopedia of NMR, Wiley, Chichester, 1996.
[2] K. Wüthrich, NMR of Proteins and Nucleic Acids, Wiley, New York, 1986.
[3] H. Kessler, M. Gehrke, C. Griesinger, Two-dimensional NMR spectroscopy: background and overview of the experiments, Angew. Chem. Int. Ed. Engl. 27 (1988) 490–536.
[4] J. Cavanagh, W.J. Fairbrother, A.G. Palmer III, N.J. Skelton, Protein NMR Spectroscopy: Principles and Practice, Academic Press, San Diego, 1996.
[5] J. Jeener, Ampere International Summer School II. Basko Polje, Yugoslavia, 1971.
[6] W.P. Aue, E. Bartholdi, R.R. Ernst, Two dimensional spectroscopy. Application to nuclear magnetic resonance, J. Chem. Phys. 64 (1976) 2229–2246.
[7] R.R. Ernst, G. Bodenhausen, A. Wokaun, Principles of nuclear magnetic resonance in one and two dimensions, Clarendon, Oxford, 1987.
[8] R.R. Ernst, W.A. Anderson, Application of Fourier transform spectroscopy to magnetic resonance, Rev. Sci. Instr. 37 (1966) 93–102.
[9] L. Frydman, T. Scherf, A. Lupulescu, The acquisition of multidimensional NMR spectra within a single scan, Proc. Natl. Acad. Sci. USA 99 (2002) 15858–15862.
[10] L. Frydman, T. Scherf, A. Lupulescu, Principles and features of single-scan two-dimensional NMR spectroscopy, J. Am. Chem. Soc. 125 (2003) in press.
[11] Y. Shrot, L. Frydman, Single-scan NMR spectroscopy at arbitrary dimensions, submitted for publication (2003).
[12] R.N. Bracewell, The Fourier Transform and its Applications, McGraw-Hill, New York, 1978.
[13] A.G. Marshall, F.R. Verdun, Fourier Transforms in NMR, Optical, and Mass Spectrometry: A User's Handbook, Elsevier, Amsterdam, 1990.
[14] L. Braunschweiler, R.R. Ernst, Coherence transfer by isotropic mixing: application to proton correlation spectroscopy, J. Magn. Reson. 53 (1983) 521–528.
[15] M. Levitt, Spin Dynamics, Wiley, New York, 2001.
[16] A.J. Shaka, J. Keeler, Broadband spin decoupling in isotropic liquids, Prog. Nucl. Magn. Reson. Spectrosc. 19 (1987) 47–129.